ELSEVIER

Fluid Phase Equilibria 172 (2000) 129–143

FLUID PHASE EQUILIBRIA

www.elsevier.nl/locate/fluid

Revision and extension of the group contribution equation of state to new solvent groups and higher molecular weight alkanes

S. Espinosa, G.M. Foco, A. Bermúdez, T. Fornari*

Planta Piloto de Ingenieria Quimica, PLAPIQUI (UNS-CONICET), Camino La Carrindanga km 7, 8000 Bahia Blanca, Argentina

Received 25 October 1999; accepted 17 May 2000

Abstract

The group contribution equation of state GC-EOS model is revised and extended. Pure group and binary interaction parameters are reported for the following new groups: ether CH_2O, ester CH_2COO/CH_3COO, chloro-aromatic ACCl and triglyceride (TG) $(CH_2COO)_2CHCOO$.

Interaction parameters between these groups and paraffin, olefin and CO_2 groups were estimated using experimental vapor–liquid equilibrium data on binary mixtures. The original aromatic-paraffinic, CO_2–paraffinic and CO_2–aromatic interaction parameters, have been revised in order to improve phase equilibrium predictions in aromatic and high molecular weight organic compounds.

Keywords: Vapor–liquid equilibria; Group contribution; Equation of state; CO_2; Triacetin; Hydrocarbons

1. Introduction

There is a large number of applications of supercritical fluids in the purification and refining of natural oils and derivatives. A recent compilation on this subject has been given by King et al. [1]. However, there is a limitation in the present thermodynamic models (mainly based on cubic equations of state) to describe the complex phase behavior, characteristic of these systems [2]. The GC-EOS model was developed by Skjold-Jorgensen [3,4] to calculate high pressure phase equilibria of non-ideal mixtures with low to medium molecular weight (lower than 300) compounds. Gros et al. [5] introduced an associating term to the original GC-EOS expression for the Helmholtz residual energy. The performance of this equation, in the correlation and prediction of phase equilibria in mixtures of near critical gases with aqueous solutions of organic compounds was greatly improved. On the other hand, infinite dilution activity coefficients (γ^{∞}) data were used to characterize the critical diameter of heavy compounds [6]. In this way, the GC-EOS

* Corresponding author. Fax: +54-291-4861600.
E-mail address: tfornari@criba.edu.ar (T. Fornari).

0378-3812/00/$20.00
PII: S0378-3812(00)00371-X

equation achieved a good correlation and prediction of vapor–liquid, liquid–liquid and liquid–supercritical fluid phase equilibria in mixtures of propane with triglycerides and natural oils.

In the present work, the GC-EOS model is revised in order to extend its application, and in particular to the representation of fluid–fluid equilibria in supercritical processes involving triglyceride and derivatives. A large variety of oils and oil derivatives can be described by a small number of functional groups, making use of the group contribution approach very efficient. For that purpose the GC-EOS parameter matrix is revised and extended, in order to include carbon dioxide, paraffinic, olefinic, aromatic, ester, ether, chloro-aromatic and triglyceride functional groups. The TG functional group was defined to characterize the three ester functions present in triglyceride. Its parameters were fitted using phase equilibrium data on mixtures containing triacetin. Good correlation and prediction of phase equilibria was obtained with the revised and extended parameter table.

The model can be applied to the simulation and development of processes for the extraction, refining, removal of pollutants, recovery of high value products, etc., of vegetable oils and derivatives using CO_2 and other gases under near critical conditions.

2. Parameterization

A brief presentation of the GC-EOS can be found in the Appendix A. For a detailed description of the model the reader is referred to the work of Skjold-Jorgensen [3,4]. The GC-EOS pure group and binary interaction parameters are described in Table 1.

The parameterization approach closely follows the procedure used by Skjold-Jorgensen [3,4]. The reference temperature T^* is assumed to be equal to 600 K for the paraffinic and hydrocarbon functional groups, and $T^*=T_c$ (critical temperature) for gases. The surface parameter q is obtained as in the UNIFAC model [7]. The critical hard sphere diameter d_c (a molecular parameter) is calculated from critical properties (gases) or using an experimental vapor pressure data point (solvents).

The attractive energy group parameters g^*, g' and g'' are estimated from vapor pressure data of pure compounds [8]. For all the groups investigated in this work, it was found that a linear temperature dependence of g is adequate (i.e. $g''=0$). The binary interaction parameters of solvent groups (k_{ij} and α_{ij}) were estimated by fitting simultaneously vapor pressure and phase equilibrium data of binary mixtures. In order to keep the number of parameters as low as possible (and if there was no significant improvement in reproducing experimental data) the following fitting policy was adopted:

- the same values of binary interaction parameters are applied to members of the same family of functional groups; for example CH_3 and CH_2, CH_3COO and CH_2COO, AC and ACH;
- the k_{ij} binary interaction parameter is non-temperature dependent;
- the non-randomness parameter α_{ij} is symmetric.

Table 1
Parameters of the GC-EOS model

Parameter for the repulsive term	d_c (critical hard sphere diameter)
Parameters for the attractive term	T^*, q, g^*, g', g'' (pure group parameters)
	k^*_{ij}, k'_{ij} α_{ij}, α_{ji} (interaction parameters)

3. Results

The CO_2–alkane systems exhibit vapor–liquid, liquid–liquid and liquid-supercritical fluid phase equilibria at high pressures. The accuracy of the GC-EOS VLE predictions worsened with the increase of the alkane carbon number, when using the original CO_2–paraffinic group interaction parameters. This was to be expected because the original parameters [4] were estimated from information on C_4–C_{10} alkanes. These binary interaction parameters were therefore readjusted to cover the range C_4–C_{28} alkanes. The same behavior was observed in mixtures of aromatic compounds with heavy alkanes. The revised parameters for these interactions and the new interactions parameters estimated in this work, are given in Table 2. References to the experimental data used for each binary interaction are given in Table 3. Table 4 contains a comparison between predictions and experimental data for CO_2 and alkane and benzene and alkane binary systems, using the original and revised parameters. The new interaction parameters maintain the original quality in the phase equilibria modeling of mixtures of CO_2 or benzene with low molecular weight alkanes (C_4–C_{10}) while the predictions for CO_2 or benzene with heavy alkanes (see Figs. 1 and 2) are significantly improved.

The correlation of VLE data of paraffinic and olefinic compounds with esters, ethers and chloro-aromatics are in good agreement with experimental data (Figs. 3–5). Equally good agreement is found for mixtures of CO_2 with these compounds (Figs. 6 and 7). Other parameters required to obtain the results shown in the figures were obtained from the literature [4,9,10].

When the definition and parameters of a monoester group is extended to the prediction of vapor pressures of triacetin, a gross deviation with experimental data is observed (Fig. 8). Taking into account that proximity effects can modify the character of the ester group in a triglyceride molecule, it was considered necessary to introduce a new TG group ($(CH_2COO)_2CHCOO$). Experimental vapor pressures and phase equilibrium data on mixtures containing triacetin (molecular weight=218) were used to fit pure group and binary interaction parameters for the TG group. Since experimental VLE data of mixtures containing triacetin is scarce, binary interaction parameters between triacetin and other solvent groups were obtained mainly from experimental γ^{∞} of a considerable number of solutes in triacetin [11,12]. Fig. 9 shows the correlation of infinite dilution activity coefficients of some of this solutes (*n*-hexane, 1-hexene, ethylacetate and ethylether) in triacetin as a function of temperature.

4. Comparison of the GC-EOS with EOS/G^E models

The main feature of the so-called EOS/G^E equations is the addition of excess Gibbs free energy (G^E) models into the mixing rule expressions for the attractive term of cubic equations of state. It is of special interest the use of the group contribution UNIFAC G^E model, in order to use the equations of state as a predictive tool.

The objective of this section is the comparison of EOS/G^E models with the GC-EOS equation in phase equilibria modeling. A comparison for mixtures containing associating compounds was made by Gross et al. [55]. In this work two well-known EOS/G^E models are compared with the GC-EOS in the prediction of phase equilibria of non-polar systems with increasing size differences. The models considered are:

1. MHV2 [56]: is a second-order approximation of the modified Huron–Vidal mixing rule [57] applied to the Soave–Redlich–Kwong (SRK) EOS with the modified UNIFAC model [58].
2. PSRK [59]: is a first-order approximation of the modified Huron–Vidal mixing rule [57] applied to the SRK EOS with the original UNIFAC model [60].

Table 2
New GC-EOS parameters

Group	Pure group parameters				
	T^* (K)	q	g^*	g'	g''
Triglyceride (TG) $(CH_2COO)_2CHCOO$	600	3.948	346350	−1.3460	0
Dimethylether (DME)	400.1	1.936	549490	−0.5091	0
Ether (CH_2O)	600	0.780	503700	−0.9821	0
Ester (CH_3COO)	600	1.728	831400	−1.0930	0
Ester (CH_2COO)	600	1.420	831400	−1.0930	0
ACCl	600	0.844	881900	−0.8453	0

Binary interaction parameters

i	j	k^*_{ij}	k'_{ij}	α_{ij}	α_{ji}
TG	CH_3/CH_2	0.860	0	0	0
	CH=CH	0.883	0	0	0
	CH_3COO/CH_2COO	1.237	0	−8.700	−3.656
	CO_2	1.094	0.1120	−1.651	−1.651
	DME/CH_2O	1.233	0.1500	0	0
	ACH/AC	0.986	0	0	0
	ACCl	1.233	0.1	−19.201	−19.201
Ether	CH_3	0.924	−0.0564	0	0
	CH_2	0.935	−0.0613	0	0
	CO_2	1.042	0	0	0
DME	CH_3	0.924	−0.0564	0	0
	CH_2	0.935	−0.0613	0	0
	Methane	1.004	−0.0564	0	0
Ester (CH_3COO/CH_3COO)	CH_3/CH_2	0.869	0	0	0
	CH=CH	1.006	0	−0.876	−0.876
	Ethane	0.800	0	0	0
	CO_2	1.115	0.0940	−1.615	−1.615
CO_2	CH_3	0.898	0	4.683	4.683
	CH_2	0.874	0	4.683	4.683
	ACCl	0.986	0.1845	−0.488	−0.488
AC	CH_3/CH_2	0.8544	0	0	0
	CH=CH	1.1	0	0	0
ACH	CH_3	0.937	0.02	−0.794	−0.794
	CH_2	1.136	0.02	−2.678	−2.678
	ACCl	1.037	0.1210	3.440	3.440
	CH=CH	1.1	0	0	0
ACCl	CH_3/CH_2	1.006	0	0	0
	CH=CH	1.286	0	0	0

Table 3
Reference for the experimental phase equilibrium data used in the regression of the parameters shown in Table 2

i	*j*	Type of experimental data used[a]	Reference
TG	CH_3/CH_2	VP data of pure triacetin and γ^∞ data of normal alkanes in triacetin	[13,14]
	CH=CH	γ^∞ data of 1-hexeno in triacetin	[14]
	Ester	γ^∞ data of ethyl-acetate in triacetin, tripalmitin, triolein and trilinolein	[12]
	CO_2	Low pressure solubility of CO_2 in triacetin	[15]
	CH_2O	γ^∞ of ethylether and butylether in triacetin	[12]
	ACH	γ^∞ of benzene in triacetin, tricaprylin, trimyristin tripalmitin and tristearin	[11,12]
	ACCl	γ^∞ of chlorobenzene in triacetin, tripalmitin, trilinolein and triolein	[11,12]
Ether	CH_3/CH_2	VP data of ethylether and butylether VLE data of the mixtures: propylether+ octane or nonane and butylether+heptane	[16]
	CO_2	VLE data of ethylether+CO_2 and butylether+CO_2 mixtures	[17,18]
DME	CH_3/CH_2	VP data of pure DME and VLE data of butane+DME mixture	[19]
	Methane	VLE data of methane and DME mixture	[20]
Ester	CH_3/CH_2	VP data of various alkyl-acetates (ethyl-butanoate, methyl-propanoate, ethyl-propanoate) and VLE data of these esters in mixture with *n*-alkanes	[13,21,22]
	CH=CH	VLE data of methylacetate+vinylacetate mixture VLE data of ester+ alkenes (hexene, octene, decene) mixtures	[23,24]
	Ethane	VLE data of methylacetate+ethane	[25]
	CO_2	High pressure VLE data of methylacetate+CO_2 and ethylacetate+CO_2 mixtures	[17,26]
CO_2	CH_3/CH_2	VLE data of *n*-alkanes (C_4–C_7)+CO_2 mixtures	References in Table 4
	ACCl	VP data of pure chlorobenzene and o-dichlorobenzene High pressure VLE data of CO_2+chlorobenzene and CO_2+*o*-dichlorobenzene mixtures	[13,27]
AC	CH_3/CH_2	VLE data of naphthalene and tetradecane mixtures	[28]
ACH	CH_3/CH_2	VLE data benzene+octane and benzene+dodecane mixtures	References in Table 4
	ACCl	Low and high pressure solubilities and VLE data of benzene in chlorobenzene	[29,30]
	CH=CH	VLE data of benzene+alkene (1-hexene, 1-heptene and 1-octene) mixtures	[31–33]
ACCl	CH_3/CH_2	VLE data of binary mixtures containing chlorobenzene with pentane, hexane or heptane	[34–36]
	CH=CH	VLE data of 1-pentene+chlorobenzene mixture	[36]

[a] VP: vapor pressure; VLE: vapor–liquid equilibria; γ^∞: infinite dilution activity coefficient.

The models mentioned above have been used in this work in the same way as suggested in the original publications; i.e. with the same pure component EOS parameters, the same UNIFAC version and with a linear mixing rule for the covolume parameter.

The MHV2 and PSRK models have been extensively compared in the literature [61,62]. These models have been quite successful in the VLE prediction of systems with components of similar size. Figs. 2–7 show a comparison between the MHV2 and GC-EOS models in the VLE modeling of non-polar systems. These results show that both models are adequate to describe the VLE in mixtures of components of low molecular weight and similar molecular size.

Table 4
Comparison between experimental VLE phase equilibrium data and GC-EOS calculations using original or revised parameters for the mixtures

Alkane	T range (K)	P range (MPa)	N[a]	STD%[b] original parameters $\times(CO_2)$	STD%[b] revised parameters (this work) $\times(CO_2)$	References
CO_2–normal alkanes						
Butane	311–340	0.4–8.2	61	11.6	14	[37]
Pentane	278–378	0.2–9.6	53	11.1	11.4	[38]
Hexane	313–393	0.8–11.6	39	12.7	5.2	[39]
Heptane	311–394	0.2–13.3	64	19.6	8.4	[40]
Decane	278–511	0.3–18.8	90	13.2	11.1	[41]
Hexadecane	308–343	0.7–17	76	20.9	10.2	[42]
Eicosane	323–473	5.9–34.4	22	16.2	10.6	[43]
Docosane	323–473	6–37.3	31	14.3	6.3	[43]
Tetracosane	373–473	0.6–31.1	34	16.1	8.3	[43,44]
Octacosane	373–423	9–40.9	9	8.5	3.3	[43]
Benzene–normal alkanes						
Heptane	313–353	12–100	60	11.8	12	[45–47]
Octane	313–348	4–60	78	5.2	5.1	[45,48]
Decane	313	0.4–24	22	12	2.9	[45]
Dodecane	298–333	6–52	52	12.7	3.2	[49,50]
Tetradecane	308–323	0.2–36	44	15.5	4.7	[51,52]
Pentadecane	298–323	3–36	30	22	6	[53]
Hexadecane	308–353	0.4–100	69	15	5	[51,54]
Heptadecane	313–353	0.2–100	42	15.7	3.4	[54]

[a] Number of experimental data points.
[b] Standard deviation in the liquid phase mole fractions. Standard deviations corresponding to vapor phase mole fractions calculated using original or new parameters are quite similar $\mathrm{STD\%}=100\sqrt{\sum[(x_{\mathrm{exp}}-x_{\mathrm{cal}})/x_{\mathrm{exp}}]^2/N}$.

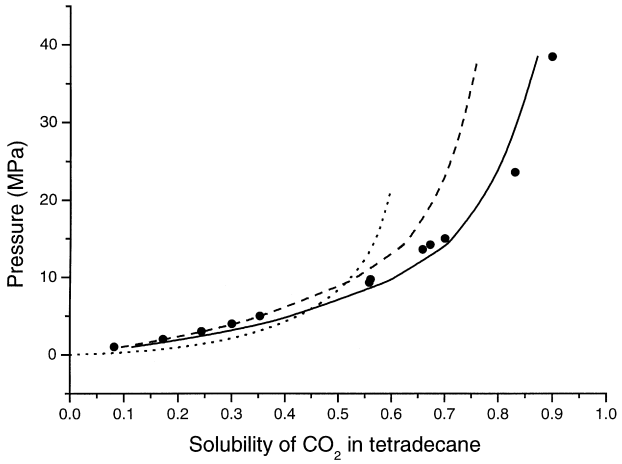

Fig. 1. VLE of CO_2+tetracosane mixture at 373 K. (●) Experimental data [43,44]; (···) MHV2; (– –) GC-EOS original parameters; (—) GC-EOS revised parameters (this work).

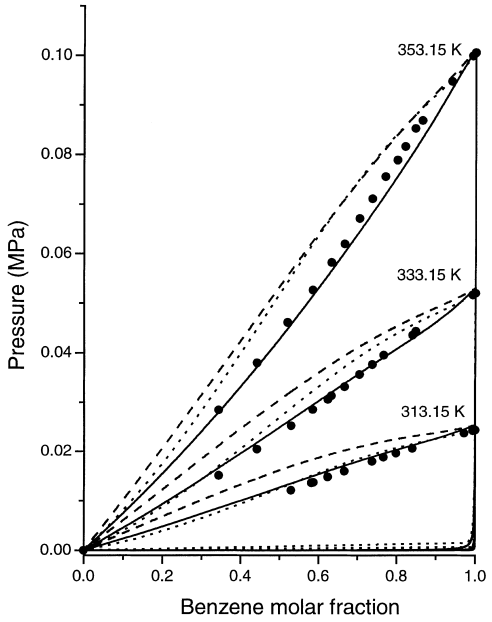

Fig. 2. VLE of benzene+heptadecane mixture. (●) Experimental data [54]; (···) MHV2; (– –) GC-EOS original parameters; (—) GC-EOS revised parameters (this work).

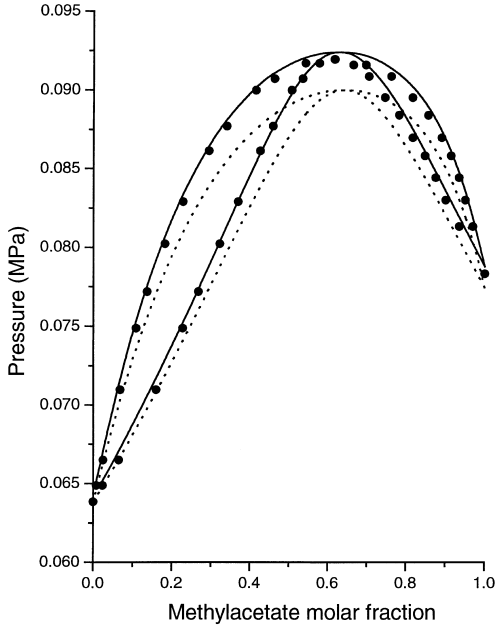

Fig. 3. VLE of methylacetate+1-hexene at 323 K. (●) Experimental data [24]; (···) MHV2; (—) GC-EOS.

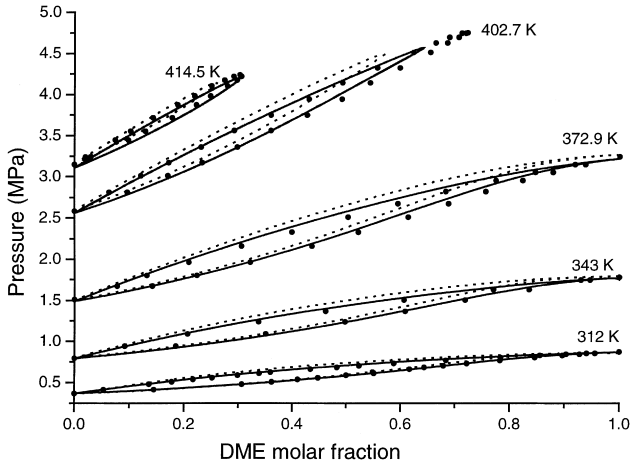

Fig. 4. VLE of DME+butane mixture. (●) Experimental data [19]; (···) MHV2; (—) GC-EOS.

The effect of increasing size differences is shown in Table 5 through a comparison between experimental VLE of mixtures of CO_2+*n*-alkanes with the MHV2, PSRK and GC-EOS predictions. The MHV2 and PSRK perform poorly when applied to very asymmetric molecular size components. The deviations of these models are greater for increasing pressures (see Fig. 1), while the GC-EOS model with revised parameters has good predictions including the high-pressure data range.

The van der Waals repulsive term of cubic EOS has been identified as a potential source of difficulties [63] in the phase equilibria modeling of size asymmetric systems. This has been attributed to the large differences in the EOS size parameters b_i. In this respect, a Carnahan–Starling repulsive term gives better results, as have been shown by Bottini et al. [6] and Peters et al. [64].

On the other hand, partial liquid–liquid miscibility is generally observed in systems with components of high differences in size. This phenomenon cannot be predicted using cubic EOS with the UNIFAC group contribution model [65].

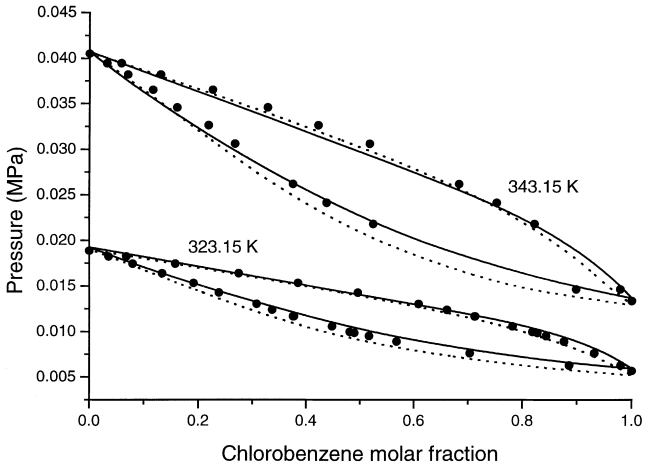

Fig. 5. VLE of chlorobenzene+heptane mixture. (●) Experimental data [35]; (···) MHV2; (—) GC-EOS.

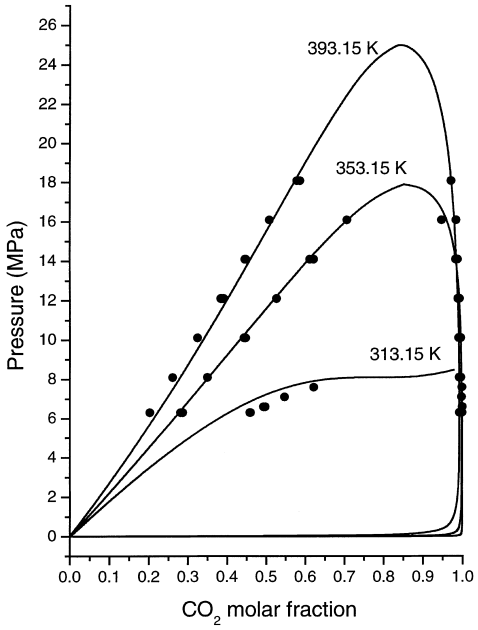

Fig. 6. VLE correlation of CO_2+*o*-dichlorobenzene mixture using the GC-EOS model. (●) Experimental data [27].

The mayor advantage of the GC-EOS model is the capability of predicting VLE and LLE with a unique set of parameters [6]. Fig. 10 shows a comparison between experimental VLE and LLE of the mixture propane and hexacontane [66] with the GC-EOS predictions. The experimental upper critical end point (UCEP) reported by Peters et al. [66] is 369.95 K. As it can be seen in the figure liquid–liquid immiscibility is predicted by the GC-EOS model at 368 K and no LLE is predicted at 397 K.

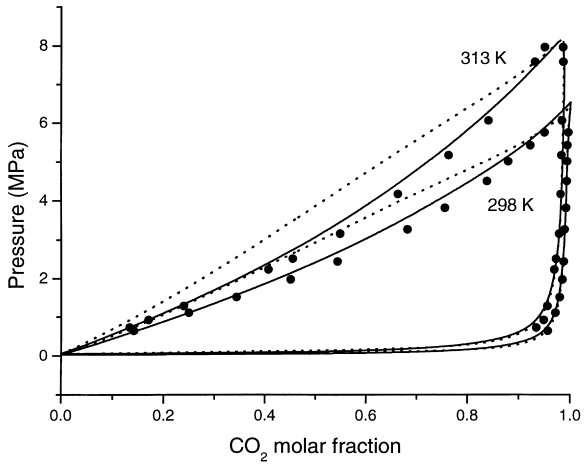

Fig. 7. VLE of CO_2+methylacetate mixture. (●) Experimental data [17]; (···) MHV2; (—) GC-EOS.

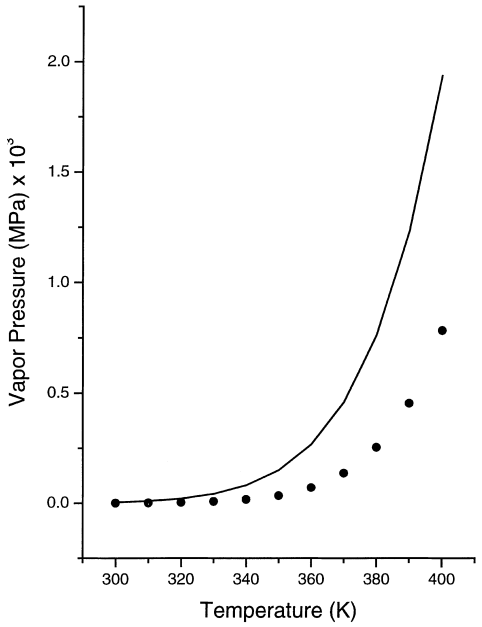

Fig. 8. Deviations in vapor pressures of triacetin using three $COOCH_3$ groups in the description of the triacetin molecule. (●) Experimental data [13]; (—) GC-EOS calculations.

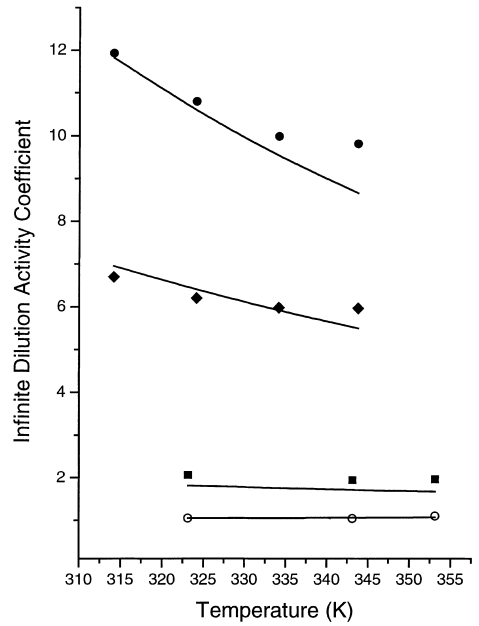

Fig. 9. GC-EOS correlation of infinite dilution activity coefficients of various solutes in triacetin. Reference for experimental data: (●) hexane [14]; (◆) 1-hexene [11]; (○) ethylacetate and (■) ethylether [12].

Table 5
Comparison between GC-EOS and EOS/G^E models in solubility predictions of carbon dioxide in high molecular weight alkanes [43]

Alkane	T range (K)	P range (MPa)	N [a]	AAD%[b] MHV2	AAD%[b] PSRK	AAD%[b] GC-EOS (this work)
Eicosane	323–473	5.9–34.4	22	25.5	18.7	8.2
Docosane	323–473	6–37.3	31	28.7	21.3	5.7
Tetracosane	373–473	9.4–31.1	20	24.6	24.5	3.9
Octacosane	373–423	9–40.8	9	28.6	28.6	2.6

[a] Number of experimental data points.
[b] Average relative deviations: AAD%=100 $\sum(|x_{exp} - x_{cal}|)/x_{exp})/N$.

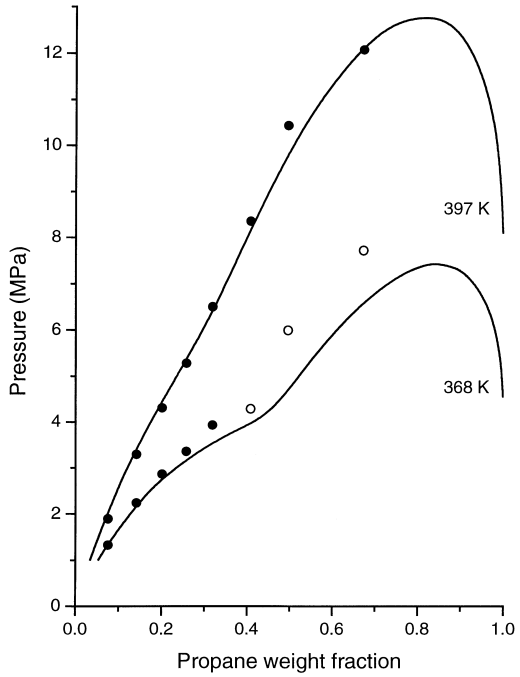

Fig. 10. Phase equilibria prediction of CO_2+hexacontane mixture using the GC-EOS model. Reference for experimental data [69]: (●) VLE; (○) LLE.

5. Conclusions

The original parameter tables for the GC-EOS have been revised and extended, including five new functional groups. The adjusted interaction parameters give a good correlation of experimental phase equilibrium data. Also, good predictions were obtained for binary and ternary mixtures not included in the parameter estimation data base. Parameters between the CO_2 and alkane groups and between aromatic (AC and ACH) and alkane groups were revised in order to obtain reliable predictions of phase equilibria of CO_2 and aromatic components, in mixtures with high molecular weight compounds.

The GC-EOS model can provide good correlation and prediction of low and high pressure VLE of mixtures with components with high differences in molecular size. The major advantage of the GC-EOS model in comparison with the EOS/G^{E} models, is the capability of predicting the partial liquid–liquid miscibility, which is experimentally observed in these type of mixtures.

Acknowledgements

The authors gratefully acknowledge financial support from the Argentine Research Council (CONICET) and the Universidad Nacional del Sur.

Appendix A

The GC-EOS model starts from the relation between the pressure and the Helmholtz energy:

$$P = -\left(\frac{\partial A}{\partial V}\right)_{T,n_i}$$

The Helmholtz energy is the sum of two parts, the first describing the ideal gas behavior and the second part is due the intermolecular forces:

$$A = A^{\text{ideal gas}} + A^{\text{residual}}$$

The residual Helmholtz energy is described by two terms: a free volume term and a contribution from attractive intermolecular forces:

$$A^{\text{residual}} = A^{\text{free volume}} + A^{\text{attraction}}$$

The free volume contribution is calculated by assuming that the molecules behave like hard spheres, characterizing each substance i by a hard sphere diameter d_i. A Carnahan–Starling type of hard sphere expression is adopted:

$$A^{\text{free volume}} = 3\left(\frac{\lambda_1\lambda_2}{\lambda_3}\right)(Y-1) + \left(\frac{\lambda_2^3}{\lambda_3^2}\right)(+Y^2 - Y - \ln Y) + n_{\mathrm{T}} \ln Y$$

with

$$Y = \left(1 - \frac{\pi\lambda_3}{6V}\right)^{-1}, \qquad \lambda_K = \sum_j^{N_{\mathrm{C}}} n_j d_j^K, \qquad n_{\mathrm{T}} = \sum_i^{N_{\mathrm{C}}} n_i$$

where n_i is the number of moles of component i, N_{C} denotes the number of components and V the total volume.

The hard sphere diameter is assumed to depend on temperature:

$$d_i = 1.065655 d_{\mathrm{c}i}\left(1 - 0.12\exp\left[\frac{-2T_{\mathrm{c}i}}{3T}\right]\right)$$

The attractive part is adopted from the NRTL equation:

$$\frac{A^{\text{attraction}}}{RT} = -\frac{z}{2}\sum_{i}^{N_C} n_i \sum_{j}^{N_G} v_j^i q_j \sum_{k}^{N_G} \frac{\theta_k g_{kj} \tilde{q} \tau_{kj}/(RTV)}{\sum_1^{N_G} \theta_1 \tau_{ij}}$$

where

$$\theta_j = \left(\frac{q_j}{\tilde{q}}\right) \sum_{i}^{N_C} n_i v_j^i, \qquad \tilde{q} = \sum_{i}^{N_C} n_i \sum_{j}^{N_G} v_j^i q_j$$

$$\tau_{ij} = \exp\left[\frac{\alpha_{ij}\Delta g_{ij}\tilde{q}}{RTV}\right]$$

$$\Delta g_{ij} = g_{ij} - g_{jj}$$

z is the number of nearest neighbors (z=10), v_j^i the number of groups of type j in molecule i, q_j represents the surface parameter of group j, θ_k the surface fraction of group k, $\tilde{q}$ denotes the total number of surface segments, g_{ij} is the attraction energy parameter for interactions between groups i and j, and α_{ij} represents the NRTL non-randomness parameter. The parameters for interactions between groups depend on temperature:

$$g_{jj} = g_{ii}^*\left[1 + g_{ii}'\left(\frac{T}{T_i^*} - 1\right) + g_{ii}'' \ln\left(\frac{T}{T_i^*}\right)\right]$$

where g_{ii}^* is the interaction parameter for reference temperature T_i^*.

Parameters for interaction between unlike groups are calculated from those between like groups:

$$g_{ij} = k_{ij}(g_{ii}g_{jj})^{1/2} \quad (k_{ij} = k_{ji})$$

where k_{ij} is a temperature-dependent binary interaction parameter:

$$k_{ij} = k_{ij}^*\left(1 + k_{ij}' \ln\left[\frac{2T}{T_i^* + T_j^*}\right]\right)$$

References

[1] J.W. King, G.R. List, Supercritical Fluid Technology in Oil and Lipid Chemistry, AOCS Press, Illinois, 1996.
[2] J.C. de la Fuente, T. Fornari, E.A. Brignole, S.B. Bottini, Supercritical Fluids: Extraction and Pollution Prevention, American Chemical Society, Washington, DC, 1997, Chapter 3, pp. 51–57.
[3] S. Skjold-Jorgensen, Fluid Phase Equilibria 16 (1984) 317–353.
[4] S. Skjold-Jorgensen, Ind. Eng. Chem. Res. 27 (1988) 110–118.
[5] H.P. Gros, S.B. Bottini, E.A. Brignole, Fluid Phase Equilibria 116 (1996) 535–544.
[6] S.B. Bottini, T. Fornari, E.A. Brignole, Fluid Phase Equilibria 158–160 (1999) 211–218.
[7] Aa. Fredenslund, R.L. Jones, J.M. Prausnitz, AIChE J. 21 (1975) 1086–1098.
[8] R.C. Reid, T.K. Sherwood, J.M. Prausnitz, The Properties of Gases and Liquids, 3rd Edition, McGraw-Hill, New York, 1977.
[9] J. Pusch, J. Schmelzer, Phys. Chem. 97 (1993) 597–603.
[10] A. Bamberger, J. Schmelzer, D. Walther, G. Maurer, Fluid Phase Equilibria 97 (1994) 167–189.

[11] G.M. Foco, A.M. Bermúdez, S.B. Bottini, J. Chem. Eng. Data 41 (1996) 1071–1074.
[12] G.M. Foco, A.M. Bermúdez, S.B. Bottini, in: J. Tojo, A. Arce (Eds.), Proceedings of the EQUIFASE'99, Vigo, Spain, 20–24 June 1999, pp. 268–273.
[13] T.E. Daubert, R.P. Danner, Physical and Thermodynamic Properties of Pure Chemicals: Data Compilation, Hemisphere, London, 1989.
[14] C. Din, G.M. Foco, T. Fornari, S.B. Bottini, Latin Am. Appl. Res. 25 (1995) 243–247.
[15] S.F. Shakhova, T.I. Bondareva, Y.P. Zubchenko, Khim. Prom. 42 (1966) 753–755.
[16] M. Venkatachalapati, G.A. Ratcliff, J. Chem. Eng. Data 17 (1972) 454–456.
[17] K. Ohgaki, T.J. Katayama, Chem. Eng. Data 20 (1975) 264–267.
[18] R.S. Mohamed, G.D. Holder, Fluid Phase Equilibria 32 (1987) 295–317.
[19] M.E. Fernández Pozo, J. Calado, J. Zollweg, W. Streett, Fluid Phase Equilibria 74 (1992) 289–302.
[20] F. García-Sanchez, S. Laugier, D. Richon, J. Chem. Eng. Data 32 (1987) 211–215.
[21] W.A. Scheller, A. Torres-Soto, K. Daphtary, J. Chem. Eng. Data 14 (1969) 17–19.
[22] B. Lu, T. Ishikawa, G.C. Benson, J. Chem. Eng. Data 35 (1990) 331–334.
[23] J. Wisniak, A. Tamir, J. Chem. Eng. Data 34 (1989) 402–404.
[24] J. Gmehling, Chem. Eng. Data 28 (1983) 27–30.
[25] K. Ohgaki, F. Sano, T.J. Katayama, J. Chem. Eng. Data 21 (1976) 55–58.
[26] L. Rusz, J. Makranczy, K.B. Megyery, L. Patyi, Hungarian J. Ind. Chem. 5 (1977) 225–232.
[27] D. Walther, G. Maurer, Ber. Bunsenges. Phys. Chem. 96 (1992) 981–988.
[28] S. Haynes, M. Van Winkle, Ind. Eng. Chem. 46 (1954) 334–338.
[29] J.R. Khurma, O.I. Muthu, S. Munjai, B.D. Smith, J. Chem. Eng. Data 28 (1983) 100–107.
[30] M. Díaz Peña, A. Compostizo, C.A. Crespo, I. Escudero, Chem. Thermodyn. 13 (1981) 869–873.
[31] J. Dojcansky, J. Heinrich, Surovy J. Chem. Zvesti 21 (1967) 713.
[32] H. Kirss, L.S. Kudryavtseva, O. Eisen, Eesti NSV Tead. Akad. Toim. Keem. Geol. 24 (1975) 15.
[33] J.H. Vera, J.M. Prausnitz, J. Chem. Eng. Data 16 (1971) 149–154.
[34] M. Rogalski, S. Malanowski, Fluid Phase Equilibria 5 (1980) 97–112.
[35] H.I. Paul, J. Krug, H. Knapp, Fluid Phase Equilibria 39 (1988) 307–324.
[36] P.J. Maher, B.D. Smith, J. Chem. Eng. Data 24 (1979) 363–375.
[37] R.H. Olds, H.H. Reamer, B.H. Sage, W.N. Lacey, Ind. Eng. Chem. 41 (1949) 475–478.
[38] G. Besserer, D.B.J. Robinson, Chem. Eng. Data 18 (1973) 416–419.
[39] Y.H. Li, K.H. Dillard, R.L.J. Robinson, J. Chem. Eng. Data 26 (1981) 53–55.
[40] H. Kalra, H. Kubota, D.B. Robinson, H.J. Ng, J. Chem. Eng. Data 23 (1978) 317–321.
[41] H. Reamer, B. Sage, J. Chem. Eng. Data 8 (1963) 508–513.
[42] A. Charoensombut-Amon, R. Martin, R. Kobayashi, Fluid Phase Equilibria 31 (1986) 89–104.
[43] Y. Sato, Y. Tagashira, D. Maruyama, S. Takishima, H. Masuoka, Fluid Phase Equilibria 147 (1998) 181–193.
[44] F.N. Tsai, J.S. Yau, J. Chem. Eng. Data 35 (1990) 43–45.
[45] M. Goral, Fluid Phase Equilibria 102 (1994) 275–286.
[46] D.A. Palmer, D.B. Smith, J. Chem. Eng. Data 17 (1972) 71–76.
[47] I. Brown, A.H. Ewald, J. Aust, Sci. Res. Ser. A 4 (1951) 198.
[48] I.M. Elshayal, B.C.-Y. Lu, J. Appl. Chem. 18 (1968) 277.
[49] R.G. Rubio, J.A.R. Renuncio, M. Díaz Peña, Thermochim. Acta 65 (1983) 69.
[50] U. Messow, K.Z. Quitzsch, Phys. Chem. (Leipzig) 257 (1976) 121.
[51] R.L. Snow, J.B. Ott, J.R. Goates, K.N. Marsh, S. O'Shea, R.H. Stokes, J. Chem. Thermodyn. 18 (1986) 107.
[52] R.G. Rubio, J.A.R. Renuncio, M. Díaz Peña, J- Solution Chem. 11 (1982) 823.
[53] R.G. Rubio, J.A.R. Renuncio, M. Díaz Peña, J. Chem. Thermodyn. 14 (1982) 983–989.
[54] U. Messow, D. Schuetze, W.Z. Hauthal, Phys. Chem. (Leipzig) 257 (1976) 218.
[55] H.P. Gros, S.B. Bottini, E.A. Brignole, Fluid Phase Equilibria 139 (1997) 75–87.
[56] S. Dahl, M. Michelsen, AIChE J. 36 (1990) 1829.
[57] M. Michelsen, Fluid Phase Equilibria 60 (1990) 47.
[58] B.L. Larsen, P. Rasmussen, Aa. Fredenslund, Ind. Eng. Chem. Res. 26 (1987) 2274.
[59] T. Holderbaum, J. Gmehling, Fluid Phase Equilibria 70 (1991) 251.
[60] H.K. Hansen, P. Rasmussen, Aa. Fredenslund, M. Schiller, J. Gmehling, Ind. Eng. Chem. Res. 30 (1991) 2352.

[61] V. Epaminondas, N. Spiliotis, N.S. Kalospiros, D. Tassios, Ind. Eng. Chem. Res. 34 (1995) 681–687.
[62] C.V. Epaminondas, C. Boukouvalas, N.S. Kalospiros, D. Tassios, Fluid Phase Equilibria 116 (1996) 480–487.
[63] R.A. Heidemann, S.L. Kokal, Fluid Phase Equilibria 56 (1990) 17–37.
[64] C.J. Peters, J.L. de Roo, J. de Swaan Arons, Fluid Phase Equilibria 72 (1992) 251–266.
[65] Aa. Fredenslund, J.M. Sørensen, in: S.I. Sandler (Ed.), Models for Thermodynamic and Phase Equilibria Calculations, Marcel Dekker, New York, 1994, pp. 287–361.
[66] C.J. Peters, J.L. de Roo, J. de Swaan Arons, Fluid Phase Equilibria 85 (1993) 301–312.